8-2017

Cross-Linked Micelles with Enzyme-Like Active Sites for Biomimetic Hydrolysis of Activated Esters

Lan Hu
Iowa State University

Yan Zhao
Iowa State University, zhaoy@iastate.edu

Cross-Linked Micelles with Enzyme-Like Active Sites for Biomimetic Hydrolysis of Activated Esters

Abstract

Enzymes have substrate-tailored active sites with optimized molecular recognition and catalytic features. Although many different platforms have been used by chemists to construct enzyme mimics, it is challenging to tune the structure of their active sites systematically. By molecularly imprinting template molecules within doubly cross-linked micelles, we created protein-sized nanoparticles with catalytically functionalized binding sites. These enzyme mimics accelerated the hydrolysis of activated esters thousands of times over the background reaction, whereas the analogous catalytic group (a nucleophilic pyridyl derivative) was completely inactive in bulk solution under the same conditions. The template molecules directly controlled the size and shape of the active site and modulated the resulting catalyst's performance at different pHs. The synthetic catalysts displayed Michaelis–Menten enzymatic behavior and, interestingly, reversed the intrinsic reactivity of the activated esters during the hydrolysis.

Keywords

Micelle, Nanoparticles, Catalysis, Molecular imprinting, Hydrolysis

Disciplines

Chemistry | Nanoscience and Nanotechnology

Article Type: Full Paper

Cross-Linked Micelles with Enzyme-Like Active Sites for Biomimetic Hydrolysis of Activated Esters

Lan Hu and Yan Zhao*

Department of Chemistry, Iowa State University, Ames, Iowa 50011-3111, zhaoy@iastate.edu

Enzymes have substrate-tailored active sites with optimized molecular recognition and catalytic features. Although many different platforms have been used by chemists to construct enzyme mimics, it is challenging to tune the structure of their active sites systematically. By molecularly imprinting template molecules within doubly cross-linked micelles, we created protein-sized nanoparticles with catalytically functionalized binding sites. These enzyme mimics accelerated the hydrolysis of activated esters thousands of times over the background reaction, whereas the analogous catalytic group (a nucleophilic pyridyl derivative) was completely inactive in bulk solution under the same conditions. The template molecules directly controlled the size and shape of the active site and modulated the resulting catalyst's performance at different pHs. The synthetic catalysts displayed Michaelis–Menten enzymatic behavior and, interestingly, reversed the intrinsic reactivity of the activated esters during the hydrolysis.

Keywords: micelle • nanoparticles • catalysis • molecular imprinting • hydrolysis

Introduction

Enzymes perform difficult catalytic tasks such as selective amide hydrolysis, C-H activation, and nitrogen fixation, all under physiological conditions. Because of their high specificity, enzymes can perform reactions at a molecular site while more reactive sites in the same molecule stay intact. When multiple functional groups of the same type (e.g., amide) exist, enzymes can selectively convert a particular one without the need of protective/deprotective chemistry, a feature highly desirable in synthesis.

The active site of an enzyme is where the selective catalysis takes place. To catalyze the intended transformation, an active site needs to have not only the appropriate functionalities for the catalysis but also molecular recognition features to bind the substrate and release the product. The polarity, acidity/basicity, and electrostatic field of the active sites, which can be very different from those of the bulk aqueous solution, also contribute to the rate acceleration.

The extraordinary catalytic properties of enzymes have prompted chemists to prepare synthetic analogues to understand their catalytic mechanisms and develop biomimetic catalysts. One way of doing this is to use synthetic foldamers[1-5] similar to peptides and proteins that fold into a convergent space, forming an active site as a result. The benefit of this approach is that catalytic functionalities can be encoded in the primary sequence and the type of building blocks, as long as the chain folds properly.[6-10] Another benefit is that environmental responsiveness can be rationally designed through conformational control of the foldamer.[11]

Catalytic active sites can be also constructed by installing catalytic groups on macrocycles.[12-13] such as cyclodextrins[14-17] and cavitands.[18-20] These macrocycles often possess well-defined binding sites with predictable molecular recognition properties. Nonetheless, since most macrocycles have fixed structures and tend to be highly symmetrical, it can be difficult to tune the shape of the binding site to match an arbitrary substrate.

Molecular imprinting creates tailored binding sites for a wide variety of molecules. Since functional monomers and cross-linkers are polymerized around the template molecules through "chemical molding" in this method, the resulting molecularly imprinted polymer (MIP) naturally contain binding sites complementary to the templates in size, shape, and binding functionality.[21-31] The method works well for many templates ranging from small drug

molecules to large biomolecules and even viruses and bacteria. Enzyme-like MIPs with functionalized active sites have also been created for selected chemical reactions.[22, 32]

We recently reported a method to molecularly imprint within cross-linked micelles.[33] Because polymerization and cross-linking are confined within the boundary of surfactant micelles, we could obtain protein-sized nanoparticles 4–5 nm in size. These molecularly imprinted nanoparticles (MINPs) have a hydrophobic/hydrophilic core–shell morphology and are fully water-soluble. We have demonstrated micellar imprinting with different types of templates including bile salt derivatives,[33] aromatic carboxylates and sulfonates,[34-36] nonsteroidal anti-inflammatory drugs (NSAIDs),[37] carbohydrates,[38-39] and peptides.[40] Because MINPs resemble proteins in size (40–60 KD in MW) and contain well-defined binding sites, we could study their binding by spectroscopic and calorimetric techniques used for molecular receptors.

In this paper, we report that the MINP binding sites could be functionalized with catalytic functionalities. The modified binding sites mimic enzyme active sites and could bind the appropriate substrates and catalyze their transformation. Importantly, our method made it possible to modify the size, shape, and depth of the binding pocket to fine tune the catalysis. The catalytic MINPs displayed Michaelis–Menten enzymatic behavior and, most interestingly, displayed selectivity contrary to what intrinsic reactivity had predicted in the hydrolysis of activated esters.

Results and Discussion

Design and Syntheses MINP-DMAP Catalysts

Despite the tremendous potential of molecular imprinting, a number of issues exist with conventional MIPs. For noncovalently imprinted materials, binding sites frequently are heterogeneous and poorly defined in structure.[21-23, 25-29, 41-42] Conventional MIPs are prepared through bulk polymerization, which gives intractable macroporous polymers that are difficult to study.[43] Over the years, chemists have used different approaches to overcome these difficulties, including performing imprinting on nanoparticles[44-51] and micro/nanogels.[52-57] The latter, in particular, have found applications in biomimetic catalysis.[53-56]

To obtain protein-sized imprinted nanoparticle, we used cross-linked micelles as a platform for molecular imprinting.[35] As shown in Scheme 1, 12-(methacryloyloxy)-*N*,*N*,*N*-tri(prop-2-yn-1-yl)dodecan-1-aminium bromide (**1**) has a tripropargylammonium headgroup and a methacrylate at the end of the hydrocarbon tail. The cationic micelle readily incorporates anionic guest such as sodium 5-(4-((4-(1-(methacryloyloxy)ethyl)-2-methoxy-5-nitrophenoxy)methyl)-1H-1,2,3-triazol-1-yl)naphthalene-1-sulfonate (**2**) by hydrophobic and electrostatic interactions. The propargyl groups allow the micelle to be cross-linked on the surface by the alkyne–azide click reaction using 1,4-diazidobutane-2,3-diol (**3**) to afford the surface-cross-linked micelle (SCM).[58-59] The SCM contains unreacted alkynes because of the 1:1.2 ratio used in the synthesis between the tris-alkyne-functionalized cross-linkable surfactant and diazide cross-linker. The click reaction also allows us to decorate the SCM with sugar-derived azido ligand *N*-(2-azidoethyl)-2,3,4,5,6-pentahydroxyhexanamide (**4**). Afterwards, thermally initiated radical polymerization among the methacrylate groups (of **1** and **2**) and divinylbenzene (DVB) solubilized by the micelle cross-links the hydrophobic core of the micelle. The 1:1 stoichiometry between **1** and DVB gives a very high cross-linking density in the core. At this point, template **2** is covalently attached to the micelle; its sulfonate ensures that the molecule is anchored to the micellar surface so that the ionic group can be properly solvated by water.

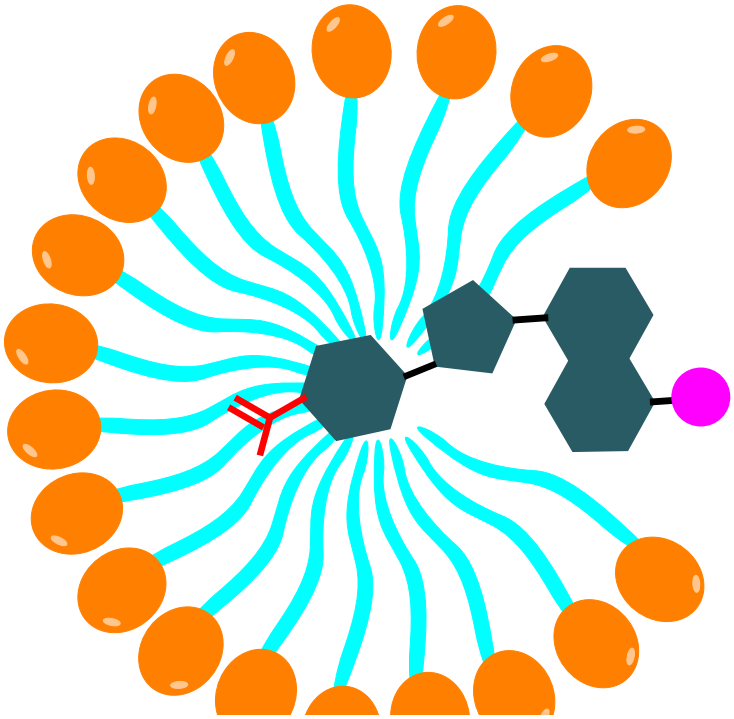

Scheme 1. Preparation of DMAP-functionalized MINP.

The template has an ortho-nitrobenzyl group, which under UV irradiation cleaves to afford a carboxylic acid and vacates the binding site. The covalent imprinting used in our procedure is expected to afford a highly template-complementary binding site with a single carboxyl group inside. In our previous work, the MINP-COOH obtained was shown to bind guest molecules that resembled the template and the carboxylic acid in the binding pocket strongly influenced the binding. Additionally, the acid could be activated by carbodiimide and chemically derivatized (by naphthylamine).[35]

In this work, we activated the carboxylic acid with 1-ethyl-3-(3-dimethylaminopropyl)carbodiimide (EDCI) following a similar procedure but treated the activated MINP-COOH with 10 equiv N^1,N^2-dimethyl-N^1-(pyridin-4-yl)ethane-1,2-diamine **5** (Scheme 1). The 10-fold excess of EDCI and amine used generally give a high conversion yield of the carboxylic acid. In our previous work, the modification of the binding site by this method afforded MINP with different binding affinities but the ITC titration showed well-behaved single-sited binding.[35] If a substantial percentage of the micelles had not been derivatized by the treatment, ITC titration would have revealed two populations of binding sites with different affinities. The pyridyl derivatize resembles 4-dimethylaminopyridine (DMAP), a powerful transacylation catalyst.[60-62] In addition to the original template **2**, we created DMAP-functionalized MINPs using analogues sodium 6-(4-((4-(1-(methacryloyloxy)ethyl)-2-methoxy-5-nitrophenoxy)methyl)-1H-1,2,3-triazol-1-yl)naphthalene-2-sulfonate (**6**) and sodium 4-(4-((4-(1-(methacryloyloxy)ethyl)-2-methoxy-5-nitrophenoxy)methyl)-1H-1,2,3-triazol-1-yl)benzoate (**7**). Although a carboxylate instead of sulfonate was used (due to availability of the starting material) in template **7**, we do not expect a significant difference from this particular change. As we have shown in previous studies,[33-34] these anionic groups mainly serve as hydrophilic anchors to stay on the surface of the micelle to ion-pair with the ammonium headgroup of the surfactant. The internal binding pocket of MINP was formed from the removal of the hydrophobic moiety of the template. The different templates thus should afford active sites with different size and shape but the same catalytic group. We refer to these catalytic cross-linked micelles as MINP(**2**)-DMAP, MINP(**6**)-DMAP, and MINP(**7**)-DMAP, respectively, with the number indicating the template used to prepare the MINP.

The surface-cross-linking and core-polymerization of the micelles were monitored by ^{1}H NMR spectroscopy. ^{1}H NMR spectroscopy normally shows broadening/disappearance of characteristic signals as the surfactant and DVB (core-cross-linker) undergo the click reaction and/or polymerization. The surface cross-linking chemistry previously was also confirmed by mass spectrometry when the 1,2-diol group of the diazide cross-linker was cleaved.[58, 63] Photocleavage of templates followed the same procedure as before and shown to be highly effective.[35] Dynamic light scattering (DLS) affords the hydrodynamic size of the MINPs. We normally keep a 50:1 ratio between the cross-linkable surfactant and the template. Since the cross-linked micelles

contained ca. 50 surfactants in the structure, the stoichiometry translates to one binding site per MINP on average, which was confirmed by multiple binding studies previously.[33-38]

Ester Hydrolysis Catalyzed by MINP-DMAPs

Our DMAP-functionalized MINPs have a hydrophobic binding site with an internal nucleophilic catalyst. The binding site was created from an aromatic group (i.e., substituted naphthyl sulfonate or benzoate) and has the nucleophilic pyridyl in the far end of the binding site. The model reaction we used to study these catalytic MINPs is the hydrolysis of *para*-nitrophenyl hexanoate (PNPH), an activated ester with a good leaving group. Its hydrophobicity will afford significant (hydrophobic) driving force for the substrate to enter the MINP binding site. Because the binding site is on the surface of the MINP (due to the anchoring effect of the sulfonate/carboxylate group on the templates), water is expected to enter the binding site fairly easily to hydrolyze the intermediate formed by the nucleophilic attack of the pyridyl on PNPH.

The pK_a of protonated DMAP is 9.7 in water,[60] suggesting that the catalyst is only active under fairly basic conditions. Indeed, when 50 μM of PNPH was incubated in HEPES buffer (pH 8.0) at 40 °C, very little hydrolysis occurred with or without DMAP in the solution. Thus, the background reactivity of PNPH and the catalytic effect of DMAP in bulk solution were negligible under this condition. As shown by Figure 1, at the same concentration of the pyridyl ligand, MINP(**2**)-DMAP catalyzed the PNPH hydrolysis powerfully, shown by the quick increase of absorbance at 400 nm from *para*-nitrophenolate formed during the reaction (Figure 1).

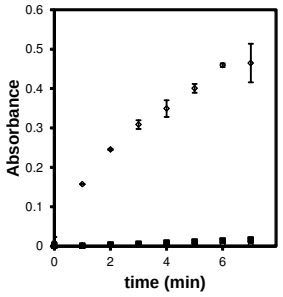

Figure 1. Absorbance at 400 nm as a function of time for the hydrolysis of PNPH in a 25 mM HEPEs buffer (pH 8.0) at 40 °C. The data sets correspond to hydrolysis in the absence of catalysts (▲) and catalyzed by DMAP (□) and MINP(**2**)-DMAP (◇), respectively. [PNPH] = 50 μM. [DMAP] = 15 μM.

We obtained the pseudo first order rate constant from the kinetic experiment and repeated the experiments for all three MINPs. In addition, we performed the hydrolysis at three different pHs to understand how the catalysts respond to environmental changes. The data are summarized in Table 1. Among the three catalysts, MINP(**7**)-DMAP seemed to be the worst and MINP(**6**)-DMAP the best. The trend stayed more or less the same at all three pHs but was most prominent at pH 6. Since DMAP itself in the bulk solution was inactive under these conditions, the observed reactivity came from the catalytic hydrolysis. It is reasonable that reactivity diminished as the pH decreased: a lower pH not only leads to protonation/deactivation of the nucleophilic catalyst (the pyridyl nitrogen), but also reduces the concentration of hydroxide, the active nucleophile.

Table 1. Rate constants for the hydrolysis of PNPH.[a]

Entry	pH	MINP(**2**)-DMAP (min^{-1})	MINP(**6**)-DMAP (min^{-1})	MINP(**7**)-DMAP (min^{-1})
1	8	0.13 ± 0.01	0.16 ± 0.02	0.14 ± 0.003
2	7	0.100 ± 0.003	0.11 ± 0.03	0.065 ± 0.005
3	6	0.017 ± 0.002	0.04 ± 0.01	0[b]

[a] The reaction rates were measured in 25 mM HEPEs buffer at 40 °C. The measurements were performed in duplicates. [b] The reaction was too slow to be measured accurately.

Because of the low background reaction under our experimental conditions, we could not determine the exact extent of rate acceleration. Comparison with our previously determined value (measured at a much higher PNPH concentration)[64] suggests that the MINP-DMAPs were thousands of times more active than DMAP in solution. The results are reasonable for DMAP located in a hydrophobic microenvironment. Molecular DMAP easily gets protonated (and deactivated) under our experimental conditions (pH 6–8) because the product, the pyridinium salt, is well solvated by water in the bulk solution. When it is located in the hydrophobic pocket inside the MINP, protonation is much more difficult and the catalytic group remains active. This is a common strategy used by enzymes to alter the pK_a values of their binding and catalytic groups. Generally, because an ionic group is better

solvated by polar solvents, environmental hydrophobicity inhibits protonation of amines and deprotonation of carboxylic acids.[65] In our previous study, environmental hydrophobicity was found to raise the pK_a of the carboxyl group from 4–5 in solution to ~6.2 inside the MINP.[35]

Figure 2 normalizes the reaction rate constants of each MINP-DMAP to its value at pH 8.0. The comparison removes the difference in intrinsic activity and shows the relative performance of individual MINP-DMAP catalysts as a function of pH. Our data shows that, overall speaking, MINP(**6**)-DMAP seemed to be the most resistant toward pH deactivation. For example, a decrease of pH from 8 to 6 eliminated the activity of MINP(**7**)-DMAP and lowered the activity of MINP(**2**)-DMAP to 13%. With the same change, MINP(**6**)-DMAP retained 23% of its activity at pH 8.

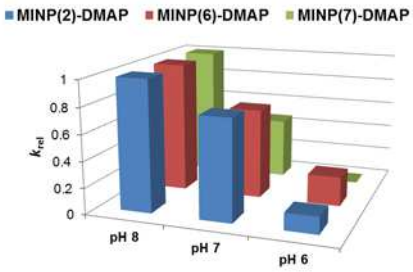

Figure 2. Relative rate constants of hydrolysis of PNPH catalyzed by the three different MINP-DMAP catalysts.

The biggest difference between the three MINPs is in the size and shape of the binding site. Templates **2** and **6** both contain a naphthyl group. The sulfonate has to stay on the micellar surface during imprinting and rebinding because of its strong solvation by water and interaction with the cationic ammonium head group of the cross-linkable surfactant. Assuming the rest of the molecule can move freely inside the micelle due to its hydrophobicity, template **6** should penetrate deeper into the micellar core than template **2**. After molecular imprinting, template removal, and post-functionalization, we expect that MINP(**6**)-DMAP has a narrower and deeper hydrophobic binding pocket than MINP(**2**)-DMAP. Template **7** is smaller than both **2** and **6**. The binding site created after it should be the smallest and possibly also shallowest, due to its shortest distance between the surface-anchoring (carboxylate) group and the methacrylate.

The absolute activity of each MINP-DAMP does not seem to correlate directly with the templates. Most likely, the catalytic activity reflects multiple favors including the binding affinity for the substrate that probably strongly depends on the size of the active site, the orientation of the bound substrate in the active site and its freedom of movement within, as well as its resistance toward pH deactivation. On the other hand, there seems to be a clear correlation between the pH resistance of the MNP-DMAP and the depth of the active site. According to Figure 2, MINP(**7**)-DMAP, whose DMAP group should be the closest to the micellar surface, got deactivated most easily. MINP(**6**)-DMAP overall was the most resistant toward pH deactivation and its active site is expected to be the longest and deepest, as discussed earlier.

Selectivity of MINP-DMAP Catalysts

We then studied MINP(**6**)-DMAP, our best catalyst, in detail. Figure 3 compares the hydrolysis of PNPH and *para*-nitrophenyl acetate (PNPA) in HEPES buffer at 40 °C. PNPA is more reactive in hydrolysis[64] but is smaller and less hydrophobic than PNPH. When the hydrolysis was catalyzed by MINP(**6**)-DMAP, the reactivity reversed, showing PNPH clearly favored by the MINP catalyst.

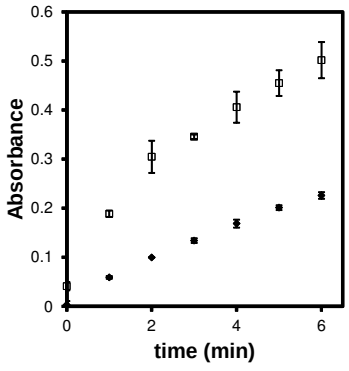

Figure 3. Absorbance at 400 nm plotted as a function of time for the hydrolysis of PNPH (□) and PNPA (◆) catalyzed by MINP(**6**)-DMAP in 25 mM HEPEs buffer (pH 8.0) at 40 °C. [PNPH] = 50 μM. [DMAP] = 15 μM. The errors were standard deviations based on three independent measurements.

Our initial hypothesis was that the reversal of activity had been caused by the stronger binding of PNPH by the hydrophobic MINP active site. To gain more understanding for the selectivity, we performed a Michaelis–Menten study on the hydrolyses.

Enzymes frequently display saturation behavior in their catalysis. The kinetics can be described by the Michaelis–Menten equation $v_o = V_{max}[S_o]/(K_m + [S_o])$, in which v_o is the initial velocity, S_o the initial substrate concentration, V_{max} the maximum velocity at a particular enzyme concentration, and K_m the Michaelis constant that measures the binding affinity of the substrate to the enzyme.[66] The Michaelis–Menten equation can be inverted to afford the Lineweaver–Burk equation, $1/v_o = K_m/V_{max} \times 1/[S_o] + 1/V_{max}$, which allows one to obtain the kinetic parameters through linear curve fitting.

As shown by Figure 4a,b, the hydrolysis of both PNPA and PNPH displayed Michaelis–Menten behavior, suggesting our MINP-DMAP catalyst indeed worked as an artificial enzyme. Table 2 summarizes the Michaelis–Menten parameters for the two substrates. We also listed the catalyst's turnover number ($k_{cat} = V_{max}$/[enzyme concentration]) and k_{cat}/K_m, which measures the catalytic efficiency. For comparison purposes, we performed similar hydrolyses catalyzed by two enzymes, bovine carbonic anhydrase (BCA) and α-chymotrypsin. These enzymes have been frequently used in the literature to catalyze the hydrolysis of *para*-nitrophenyl esters,[67-70] even though they are not natural esterases. Because the literature reports typically did not compare the two substrates under relevant conditions, we performed the kinetic experiments ourselves for the two enzymes.

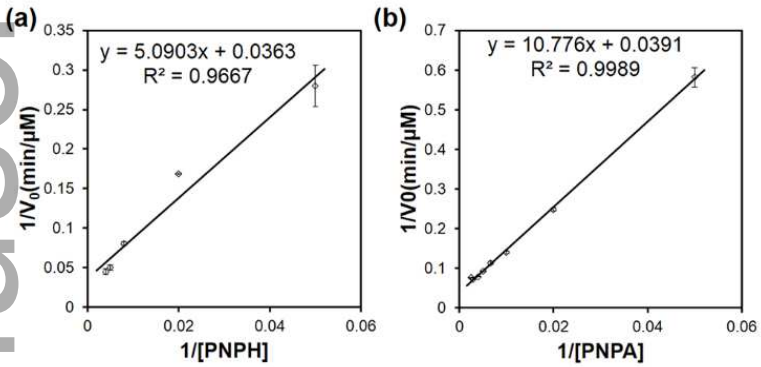

Figure 4. (a) Lineweaver-Burk plot for the hydrolysis of PNPH by MINP(**6**)-DMAP in a 25 mM HEPEs buffer at 40 °C and pH 8.0. (b) Lineweaver-Burk plot for the hydrolysis of PNPA by MINP(**6**)-DMAP in a 25 mM HEPEs buffer at 40 °C and pH 8.0. The errors were standard deviations based on three independent measurements.

Table 2. Rate constants for the hydrolysis of PNPH.[a]

Entry	catalyst	substrate	V_{max} (μM/min)	K_m (μM)	k_{cat} (min^{-1})	k_{cat}/K_m (min^{-1} mM^{-1})
1	BCA	PNPA	770 ± 120	1960 ± 350	77 ± 12	39.2 ± 1.2
		PNPH[b]	1.99 ± 0.17	230 ± 40	0.249 ± 0.021	1.10 ± 0.07
2	α-Chymotrypsin	PNPA	1000 ± 80	8550 ± 560	100 ± 8	11.7 ± 0.3
		PNPH	440 ± 50	670 ± 80	44 ± 5	64.9 ± 1.9
3	MINP(**6**)-DMAP	PNPA	24.3 ± 0.7	250 ± 12	2.43 ± 0.17	9.72 ± 0.22
		PNPH	33.9 ± 3.2	200 ± 30	3.39 ± 0.32	17.1 ± 1.3

[a] The kinetic experiments were performed in 25 mM HEPEs buffer (pH 8.0) at 40 °C. The concentration of the catalysts was 10 μM unless otherwise indicated. The errors were standard deviations based on three independent measurements. [b] [BCA] = 8.0 μM.

Our data shows that BCA is particularly selective for PNPA. The V_{max} value was hundreds of times larger than that for PNPH at the same enzyme concentration (8 μM). PNPH was clearly bound more strongly by the enzyme, as the dissociative constant K_m was only ~1/9 of that for PNPA (Table 2, entry 1). Once the binding effect (K_m) was removed, the catalytic efficiency (k_{cat}/K_m) was about 36 times higher for PNPA than for PNPH.
In comparison, α-chymotrypsin was not as nearly as selective as BCA. Although it still turns over PNPA faster, the PNPA/PNPH selectivity was only a little over two-fold. PNPH still showed a stronger binding, with its K_m being ~1/13 of that for PNPA. Once the binding effect is removed, the catalytic efficiency (k_{cat}/K_m) was higher for PNPH than PNPA. Thus, although the two enzymes both bound PNPH more strongly than PNPA, the inherent catalytic efficiencies reversed, probably as a result of different catalytic mechanisms.

The behavior of MINP(**6**)-DMAP was different. First of all, the binding selectivity was minimal—K_m was 250 μM and 200 μM for PNPA and PNPH, respectively. Thus, although PNPH was bound more strongly, the binding selectivity was far smaller than that displayed by the two enzymes. The faster reaction of PNPH, therefore, is unlikely to be caused by the binding selectivity, different from what we thought. As far as the absolute turnover number

was concerned, our MINP was the only catalyst among the three that converted PNPH faster than PNPA. This remains significant, as PNPA has a higher intrinsic activity than PNPH.

Conclusions

In this study, we have shown that, by molecular imprinting within cross-linked micelles, we can create catalytically active sites with tunable size, shape, and depth. The strategy allowed us to create artificial esterases under conditions in which the catalytic group (DMAP) is fully deactivated in the bulk solution. As a result, we could perform nucleophilic/basic catalysis under acidic conditions, a feature difficult to achieve without the supramolecular control.

Interestingly, our MINP(**6**)-DMAP catalyst displayed selectivity opposite to that of the intrinsic reactivity. The Michaelis–Menten study revealed that, although binding affinity of the substrate was important to the catalysis, the catalytic selectivity could derive from other properties even in relatively simple artificial enzymes. Our results suggest a better control of the active site is important if chemists want to construct enzyme mimics. Molecular imprinting is a very powerful method for constructing guest-specific binding pockets. With the micellar imprinting technique, we can create protein-size nanoparticles with well-defined active sites. As we develop stronger abilities to control the size, shape, and functionalities in the active sites, we should be able to construct more capable artificial enzymes for less reactive substrates with higher selectivity.

Experimental Section

General

All reagents and solvents were of ACS-certified grade or higher and used as received from commercial suppliers. Millipore water was used to prepare buffers and nanoparticles. ^{1}H and ^{13}C NMR spectra were recorded on a VARIAN MR-400 or on a VARIAN VXR-400 spectrometer. Dynamic light scattering (DLS) was performed on a PD2000DLSPLUS dynamic light scattering detector. Mass spectrometry was performed on AGILENT 6540 QTOF mass spectrometer. UV-vis spectra were recorded on a Cary 100 Bio UV-visible spectrophotometer.

Syntheses

Syntheses of compounds **1**–**4**[33] and **5**[8] were previously reported.

Sodium 6-azidonaphthalene-2-sulfonate (8): A solution of 6-amino-2-naphthalenesulfonic acid (1.50 g, 6.72 mmol) in 10 mL of concentrated sulfuric acid was stirred at -10 °C while a solution $NaNO_2$ (1.00 g, 14.50 mmol) in 8 mL of water was added dropwise. Additional 10 mL of water was added. After the reaction mixture was stirred for 45 min, sodium azide (1.00 g, 15.38 mmol) in 9 mL of water was slowly added. After the mixture was at 4 °C for 8 h, sodium chloride (12 g) was added. The precipitate formed was collected by suction filtration and quickly washed with water (2 × 15 mL) to yield a pink powder (1.57 g, 94%). ^{1}H NMR (400 MHz, DMSO, δ): 8.15 (t, J = 0.8 Hz, 1H), 8.04 (d, J = 8.8 Hz, 1H), 7.85 (d, J = 8.8Hz , 1H), 7.72 (dd, J_1 = 8.4 Hz, J_2 = 1.6 Hz, 1H), 7.67 (d, J = 2.4 Hz, 1H), 7.27 (dd, J_1 = 8.8 Hz, J_2 = 2.4 Hz, 1H).). ^{13}C NMR (100 MHz, DMSO, δ): 145.2, 138.0, 133.9, 131.1, 130.1, 127.1, 125.4, 124.6, 119.7, 116.0. ESI-HRMS (m/z): $[M\text{-}Na]^-$ calcd for $C_{10}H_6N_3O_3S$, 248.0135; found, 248.0129.

Compound 6: To an ice-cold solution of 1-(5-methoxy-2-nitro-4-(prop-2-yn-1-yloxy)phenyl)ethan-1-ol (**9**)[33] (100 mg, 0.40 mmol) and triethylamine (0.17 mL, 1.2 mmol) in anhydrous dichloromethane (20 mL), methacryloyl chloride (0.12 mL, 1.2 mmol) was added dropwise under nitrogen. The mixture was warmed to room temperature and stirred overnight. The reaction was quenched by the addition of water and extracted with ethyl acetate (2 × 10 mL). The organic layer was washed with 1 M HCl to ~pH 6 and rinsed with water (2 × 10 mL). The crude product was dried over sodium sulfate and the solvents removed in vacuo to give a clear oil. The oil obtained (30 mg, 0.09 mmol) was added to **8** (20 mg, 0.08 mmol) in a 2:1 THF/water mixture (5 mL). Sodium ascorbate (28 mg, 0.12 mmol) and copper sulfate hydrate (23 mg, 0.08 mmol) were added and the mixture was stirred at 40 °C in the dark for 12 h. The solvents were removed in vacuo and sodium chloride (10 g) was added to the concentrated mixture. The precipitate collected was rinsed with dichloromethane (10 mL), dried in air, washed with a 5:3 mixture of dichloromethane/methanol, and purified by column chromatography over silica gel using 2:1 methylene chloride/methanol as the eluent to give a yellow powder (20 mg, 44%). ^{1}H NMR (400 MHz, CD_3OD, δ): 9.13 (d, J = 8.4 Hz, 1H), 8.50 (s, 1H), 8.30 (d, J = 7.2 Hz, 1H), 7.73 (m, 2H), 7.65 (m, 3H), 7.19 (s, 1H), 6.44 (d, J = 6.8 Hz, 1H), 6.12 (d, J = 7.2 Hz, 1H), 5.67 (m, 1H), 5.43 (s, 2H), 3.94 (s, 3H), 1.94 (d, J = 6.8 Hz, 3H), 1.68 (m, 3H). ^{13}C NMR (100 MHz, CD3OD, δ): 170.3, 138.4, 128.5, 125.8, 125.8, 125.8, 123.0, 123.0, 123.0, 123.0, 120.4, 120.4, 120.4, 120.4, 119.3, 119.3, 119.3, 112.8, 112.8, 112.8, 108.0, 80.0, 72.9, 55.2, 28.9, 27.9. ESI-HRMS (m/z): $[M\text{-}Na]^-$ calcd for $C_{26}H_{23}N_4O_9S$, 567.1180; found, 567.1186.

Compound 7: The same procedure for 6 was followed using 4-azidobenzoate instead of 8. The overall yield of the reactions was 41%. ^{1}H NMR (400 MHz, DMSO, δ): 9.07 (s, 1H), 8.13 (d, *J* = 12 Hz, 2H), 8.06 (d, *J* = 8 Hz, 2H), 7.87 (s, 1H), 7.17 (s, 1H), 6.26 (q, *J* = 4.0 Hz, 1H), 6.12 (s, 1H), 5.71 (s, 1H), 5.35 (s, 2H), 3.87 (s, 3H), 1.86 (s, 3H), 1.62 (d, *J* = 8.0 Hz, 3H). ^{13}C NMR (100 MHz, DMSO, δ): 166.1, 154.0, 146.7, 143.8, 140.1, 136.1, 132.7, 126.9, 123.9, 120.4, 109.7, 109.3, 68.31, 62.32, 56.65, 21.75. ESI-HRMS (m/z): [M-Na]$^{-}$ calcd for $C_{23}H_{21}N_4O_8$, 481.1365; found 481.1359.

General procedure for the preparation of MINP-COOH: A typical procedure is as follows.[33] To a micellar solution of compound **1** (9.3 mg, 0.02 mmol) in D_2O (2.0 mL), divinylbenzene (DVB, 2.8 µL, 0.02 mmol), compound **2** in D_2O (10 µL, 0.0004 mmol), and AIBN (10 µL of a 8.2 mg/mL solution in DMSO, 0.0005 mmol) were added. (D_2O instead of H_2O was used in the preparation so that the cross-linking and polymerization of the micelles could by monitored by ^{1}H NMR spectroscopy.) The mixture was subjected to ultrasonication for 10 min before compound **3** (4.13 mg, 0.024 mmol), $CuCl_2$ (10 µL of a 6.7 mg/mL solution in D_2O, 0.0005 mmol), and sodium ascorbate (10 µL of a 99 mg/mL solution in D_2O, 0.005 mmol) were added. After the reaction mixture was stirred slowly at room temperature for 12 h, compound **4** (10.6 mg, 0.04 mmol), $CuCl_2$ (10 µL of a 6.7 mg/mL solution in D_2O, 0.0005 mmol l), and sodium ascorbate (10 µL of a 99 mg/mL solution in D_2O, 0.005 mmol) were added. After being stirred for another 6 h at room temperature, the reaction mixture was transferred to a glass vial, purged with nitrogen for 15 min, sealed with a rubber stopper, and heated at 75 °C for 16 h. The resultant solution (2 mL) was cooled to room temperature, purged with nitrogen again for 15 min, and irradiated in a Rayonet reactor for 12 h. The precipitate formed after addition of acetone (8 mL) was collected by suction filtration and washed five times with 1:4 water/acetone mixture and five times with methanol. The material was dried in air to give an off-white powder (15 mg, 75%).

General procedure for the preparation of MINP-DMAP: A typical procedure is as follows. EDCI (10 µL of a 61 mg/mL solution in dry DMF, 0.004 mmol) was added to a stirred solution of MINP-COOH (20.0 mg, 0.0004 mmol) in dry DMF (1 mL) at 0 °C under nitrogen. After 2 h, compound **5** (10 µL of a 66.1 mg/mL solution in DMF, 0.004 mmol) was added and the mixture was stirred for 24 h at room temperature. The mixture was concentrated in vacuo and poured into 2 mL of acetone. The precipitate formed was collected by centrifugation and rinsed several times with 2 mL of acetone to afford the product as an off-white powder (15 mg, 75%).

Kinetic experiments

Stock solutions of PNPH and PNPA (10.0 mM) in methanol were stored in a refrigerator and used within 3 days. A typical kinetic experiment is as follows. A 60 µM stock solution of MINP(**2**)-DMAP was prepared by dissolving of 3.0 mg of the MINP in 1.00 mL of HEPES buffer (25 mM, pH 8.0). An aliquot of this solution (500 µL) was diluted with the HEPES buffer in a cuvette to a final volume of 2.00 mL. The cuvette was placed in a UV-vis spectrometer and equilibrated to 40 °C. After 5 min, 10 µL of the PNPH stock solution was added into the cuvette. The hydrolysis was monitored by the absorbance of *para*-nitrophenoxide anion at 400 nm (or 320 nm for *para*-nitrophenol below pH7).

Supplementary Material

Supporting information for this article including aAdditional figures and NMR spectra of key compounds is available on the WWW under http://dx.doi.org/10.1002/MS-number.

Acknowledgements

We thank NSF (DMR-1464927) for financial support of this research.

References

[1] S. H. Gellman, 'Foldamers: A manifesto', *Acc. Chem. Res.* **1998**, *31*, 173-180.

[2] D. J. Hill, M. J. Mio, R. B. Prince, T. S. Hughes, J. S. Moore, 'A field guide to foldamers', *Chem. Rev.* **2001**, *101*, 3893-4012.

[3] S. Hecht, I. Huc, Wiley-VCH, Weinheim, **2007**.

[4] D.-W. Zhang, X. Zhao, J.-L. Hou, Z.-T. Li, 'Aromatic Amide Foldamers: Structures, Properties, and Functions', *Chem. Rev.* **2012**, *112*, 5271-5316.

[5] M. S. Cubberley, B. L. Iverson, 'Models of higher-order structure: foldamers and beyond', *Curr. Opin. Chem. Biol.* **2001**, *5*, 650-653.

[6] R. A. Smaldone, J. S. Moore, 'Foldamers as reactive sieves: reactivity as a probe of conformational flexibility', *J. Am. Chem. Soc.* **2007**, *129*, 5444-5450.

[7] G. Maayan, M. D. Ward, K. Kirshenbaum, 'Folded biomimetic oligomers for enantioselective catalysis', *Proc. Natl. Acad. Sci. U. S. A.* **2009**, *106*, 13679-13684.

[8] H. Cho, Z. Zhong, Y. Zhao, 'A DMAP-functionalized oligocholate foldamer for solvent-responsive catalysis', *Tetrahedron* **2009**, *65*, 7311-7316.

[9] M. M. Müller, M. A. Windsor, W. C. Pomerantz, S. H. Gellman, D. Hilvert, 'A Rationally Designed Aldolase Foldamer', *Angew. Chem. Int. Ed.* **2009**, *48*, 922-925.

[10] C. Mayer, M. M. Muller, S. H. Gellman, D. Hilvert, 'Building proficient enzymes with foldamer prostheses', *Angew. Chem. Int. Ed.* **2014**, *53*, 6978-6981.

[11] H. Cho, Y. Zhao, 'Environmental effects dominate the folding of oligocholates in solution, surfactant micelles, and lipid membranes', *J. Am. Chem. Soc.* **2010**, *132*, 9890-9899.

[12] D. M. Vriezema, M. C. Aragones, J. Elemans, J. Cornelissen, A. E. Rowan, R. J. M. Nolte, 'Self-assembled nanoreactors', *Chem. Rev.* **2005**, *105*, 1445-1489.

[13] M. Raynal, P. Ballester, A. Vidal-Ferran, P. W. N. M. van Leeuwen, 'Supramolecular catalysis. Part 2: artificial enzyme mimics', *Chem. Soc. Rev.* **2014**, *43*, 1734-1787.

[14] G. L. Trainor, R. Breslow, 'High acylation rates and enantioselectivity with cyclodextrin complexes of rigid substrates', *J. Am. Chem. Soc.* **1981**, *103*, 154-158.

[15] L. G. Marinescu, M. Bols, 'Very High Rate Enhancement of Benzyl Alcohol Oxidation by an Artificial Enzyme', *Angew. Chem. Int. Ed.* **2006**, *45*, 4590-4593.

[16] D.-Q. Yuan, Y. Kitagawa, K. Aoyama, T. Douke, M. Fukudome, K. Fujita, 'Imidazolyl Cyclodextrins: Artificial Serine Proteases Enabling Regiospecific Reactions', *Angew. Chem. Int. Ed.* **2007**, *46*, 5024-5027.

[17] S. Hu, J. Li, J. Xiang, J. Pan, S. Luo, J.-P. Cheng, 'Asymmetric Supramolecular Primary Amine Catalysis in Aqueous Buffer: Connections of Selective Recognition and Asymmetric Catalysis', *J. Am. Chem. Soc.* **2010**, *132*, 7216-7228.

[18] A. Gissot, J. Rebek, 'A Functionalized, Deep Cavitand Catalyzes the Aminolysis of a Choline Derivative', *J. Am. Chem. Soc.* **2004**, *126*, 7424-7425.

[19] S. R. Shenoy, F. R. Pinacho Crisóstomo, T. Iwasawa, J. Rebek, 'Organocatalysis In a Synthetic Receptor with an Inwardly Directed Carboxylic Acid', *J. Am. Chem. Soc.* **2008**, *130*, 5658-5659.

[20] B.-Y. Wang, T. Žujović, D. A. Turner, C. M. Hadad, J. D. Badjić, 'Design, Preparation, and Study of Catalytic Gated Baskets', *J. Org. Chem.* **2012**, *77*, 2675-2688.

[21] G. Wulff, 'Molecular Imprinting in Cross-Linked Materials with the Aid of Molecular Templates— A Way towards Artificial Antibodies', *Angew. Chem. Int. Ed. Engl.* **1995**, *34*, 1812-1832.

[22] G. Wulff, 'Enzyme-like Catalysis by Molecularly Imprinted Polymers', *Chem. Rev.* **2001**, *102*, 1-28.

[23] K. Haupt, K. Mosbach, 'Molecularly Imprinted Polymers and Their Use in Biomimetic Sensors', *Chem. Rev.* **2000**, *100*, 2495-2504.

[24] L. Ye, K. Mosbach, 'Molecular Imprinting: Synthetic Materials As Substitutes for Biological Antibodies and Receptors', *Chem. Mater.* **2008**, *20*, 859-868.

[25] K. J. Shea, 'Molecular imprinting of synthetic network polymers: the de novo synthesis of macromolecular binding and catalytic sites', *Trends Polym. Sci.* **1994**, *2*, 166-173.

[26] B. Sellergren, *Molecularly imprinted polymers: man-made mimics of antibodies and their applications in analytical chemistry*, Elsevier, Amsterdam, **2001**.

[27] M. Komiyama, *Molecular imprinting: from fundamentals to applications*, Wiley-VCH, Weinheim, **2003**.

[28] M. Yan, O. Ramström, *Molecularly imprinted materials: science and technology*, Marcel Dekker, New York, **2005**.

[29] C. Alexander, H. S. Andersson, L. I. Andersson, R. J. Ansell, N. Kirsch, I. A. Nicholls, J. O'Mahony, M. J. Whitcombe, 'Molecular imprinting science and technology: a survey of the literature for the years up to and including 2003', *J. Mol. Recognit.* **2006**, *19*, 106-180.

[30] B. Sellergren, A. J. Hall, in *Supramolecular Chemistry: From Molecules to Nanomaterials* (Eds.: J. W. Steed, P. A. Gale), Wiley, Online, **2012**.

[31] K. Haupt, C. Ayela, *Molecular Imprinting*, Springer, Heidelberg ; New York, **2012**.

[32] G. Wulff, J. Liu, 'Design of biomimetic catalysts by molecular imprinting in synthetic polymers: the role of transition state stabilization', *Acc. Chem. Res.* **2012**, *45*, 239-247.

[33] J. K. Awino, Y. Zhao, 'Protein-Mimetic, Molecularly Imprinted Nanoparticles for Selective Binding of Bile Salt Derivatives in Water', *J. Am. Chem. Soc.* **2013**, *135*, 12552-12555.

[34] J. K. Awino, Y. Zhao, 'Molecularly Imprinted Nanoparticles as Tailor-Made Sensors for Small Fluorescent Molecules', *Chem. Commun.* **2014**, *50*, 5752-5755.

[35] J. K. Awino, Y. Zhao, 'Water-Soluble Molecularly Imprinted Nanoparticles (MINPs) with Tailored, Functionalized, Modifiable Binding Pockets', *Chem.-Eur. J.* **2015**, *21*, 655-661.

[36] J. K. Awino, L. Hu, Y. Zhao, 'Molecularly Responsive Binding through Co-occupation of Binding Space: A Lock–Key Story', *Org. Lett.* **2016**, *18*, 1650-1653.

[37] J. K. Awino, Y. Zhao, 'Polymeric Nanoparticle Receptors as Synthetic Antibodies for Nonsteroidal Anti-Inflammatory Drugs (NSAIDs)', *ACS Biomater. Sci. Eng.* **2015**, *1*, 425-430.

[38] J. K. Awino, R. W. Gunasekara, Y. Zhao, 'Selective Recognition of d-Aldohexoses in Water by Boronic Acid-Functionalized, Molecularly Imprinted Cross-Linked Micelles', *J. Am. Chem. Soc.* **2016**, *138*, 9759-9762.

[39] R. W. Gunasekara, Y. Zhao, 'A General Method for Selective Recognition of Monosaccharides and Oligosaccharides in Water', *J. Am. Chem. Soc.* **2017**, *139*, 829-835.

[40] J. K. Awino, R. W. Gunasekara, Y. Zhao, 'Sequence-Selective Binding of Oligopeptides in Water through Hydrophobic Coding', *J. Am. Chem. Soc.* **2017**, *139*, 2188-2191.

[41] B. Sellergren, 'Imprinted Polymers with Memory for Small Molecules, Proteins, or Crystals', *Angew. Chem. Int. Ed.* **2000**, *39*, 1031-1037.

[42] X. Wu, W. R. Carroll, K. D. Shimizu, 'Stochastic Lattice Model Simulations of Molecularly Imprinted Polymers', *Chem. Mater.* **2008**, *20*, 4335-4346.

[43] S. C. Zimmerman, N. G. Lemcoff, 'Synthetic hosts via molecular imprinting-are universal synthetic antibodies realistically possible?', *Chem. Commun.* **2004**, 5-14.

[44] Z. Li, J. Ding, M. Day, Y. Tao, 'Molecularly Imprinted Polymeric Nanospheres by Diblock Copolymer Self-Assembly', *Macromolecules* **2006**, *39*, 2629-2636.

[45] Y. Hoshino, T. Kodama, Y. Okahata, K. J. Shea, 'Peptide Imprinted Polymer Nanoparticles: A Plastic Antibody', *J. Am. Chem. Soc.* **2008**, *130*, 15242-15243.

[46] F. Priego-Capote, L. Ye, S. Shakil, S. A. Shamsi, S. Nilsson, 'Monoclonal Behavior of Molecularly Imprinted Polymer Nanoparticles in Capillary Electrochromatography', *Anal. Chem.* **2008**, *80*, 2881-2887.

[47] A. Cutivet, C. Schembri, J. Kovensky, K. Haupt, 'Molecularly Imprinted Microgels as Enzyme Inhibitors', *J. Am. Chem. Soc.* **2009**, *131*, 14699-14702.

[48] K. G. Yang, M. M. Berg, C. S. Zhao, L. Ye, 'One-Pot Synthesis of Hydrophilic Molecularly Imprinted Nanoparticles', *Macromolecules* **2009**, *42*, 8739-8746.

[49] Z. Y. Zeng, J. Patel, S. H. Lee, M. McCallum, A. Tyagi, M. D. Yan, K. J. Shea, 'Synthetic Polymer Nanoparticle-Polysaccharide interactions: A Systematic Study', *J. Am. Chem. Soc.* **2012**, *134*, 2681-2690.

[50] Y. Ma, G. Q. Pan, Y. Zhang, X. Z. Guo, H. Q. Zhang, 'Narrowly Dispersed Hydrophilic Molecularly Imprinted Polymer Nanoparticles for Efficient Molecular Recognition in Real Aqueous Samples Including River Water, Milk, and Bovine Serum', *Angew. Chem. Int. Ed.* **2013**, *52*, 1511-1514.

[51] Y. Zhang, C. Deng, S. Liu, J. Wu, Z. Chen, C. Li, W. Lu, 'Active Targeting of Tumors through Conformational Epitope Imprinting', *Angew. Chem. Int. Ed.* **2015**, *54*, 5157-5160.

[52] A. Biffis, N. B. Graham, G. Siedlaczek, S. Stalberg, G. Wulff, 'The synthesis, characterization and molecular recognition properties of imprinted microgels', *Macromol. Chem. Phys.* **2001**, *202*, 163-171.

[53] S. C. Maddock, P. Pasetto, M. Resmini, 'Novel imprinted soluble microgels with hydrolytic catalytic activity', *Chem. Commun.* **2004**, 536-537.

[54] G. Wulff, B. O. Chong, U. Kolb, 'Soluble single-molecule nanogels of controlled structure as a matrix for efficient artificial enzymes', *Angew. Chem. Int. Ed.* **2006**, *45*, 2955-2958.

[55] D. Carboni, K. Flavin, A. Servant, V. Gouverneur, M. Resmini, 'The First Example of Molecularly Imprinted Nanogels with Aldolase Type I Activity', *Chem. -Eur. J.* **2008**, *14*, 7059-7065.

[56] A. Servant, K. Haupt, M. Resmini, 'Tuning Molecular Recognition in Water-Soluble Nanogels with Enzyme-Like Activity for the Kemp Elimination', *Chem.-Eur. J.* **2011**, *17*, 11052-11059.

[57] P. Çakir, A. Cutivet, M. Resmini, B. T. Bui, K. Haupt, 'Protein-size molecularly imprinted polymer nanogels as synthetic antibodies, by localized polymerization with multi-initiators', *Adv. Mater.* **2013**, *25*, 1048-1051.

[58] S. Zhang, Y. Zhao, 'Facile Synthesis of Multivalent Water-Soluble Organic Nanoparticles via "Surface Clicking" of Alkynylated Surfactant Micelles', *Macromolecules* **2010**, *43*, 4020-4022.

[59] H.-Q. Peng, Y.-Z. Chen, Y. Zhao, Q.-Z. Yang, L.-Z. Wu, C.-H. Tung, L.-P. Zhang, Q.-X. Tong, 'Artificial Light-Harvesting System Based on Multifunctional Surface-Cross-Linked Micelles', *Angew. Chem. Int. Ed.* **2012**, *51*, 2088-2092.

[60] G. Höfle, W. Steglich, H. Vorbrüggen, '4-Dialkylaminopyridines as Highly Active Acylation Catalysts.', *Angew. Chem. Int. Ed. Engl.* **1978**, *17*, 569-583.

[61] R. Murugan, E. F. V. Scriven, 'Applications of dialkylaminopyridine (DMAP) catalysts in organic synthesis', *Aldrichimica Acta* **2003**, *36*, 21-27.

[62] M. R. Heinrich, H. S. Klisa, H. Mayr, W. Steglich, H. Zipse, 'Enhancing the catalytic activity of 4-(dialkylamino)pyridines by conformational fixation', *Angew. Chem. Int. Ed.* **2003**, *42*, 4826-4828.

[63] X. Li, Y. Zhao, 'Protection/Deprotection of Surface Activity and Its Applications in the Controlled Release of Liposomal Contents', *Langmuir* **2012**, *28*, 4152-4159.

[64] G. Chadha, Y. Zhao, 'Environmental control of nucleophilic catalysis in water', *Chem. Commun.* **2014**, *50*, 2718-2720.

[65] D. Matulis, V. A. Bloomfield, 'Thermodynamics of the hydrophobic effect. I. Coupling of aggregation and pKa shifts in solutions of aliphatic amines', *Biophys. Chem.* **2001**, *93*, 37-51.

[66] T. Palmer, *Understanding enzymes*, 4th ed., Prentice Hall/Ellis Horwood, London ; New York, **1995**.

[67] F. J. Kezdy, M. L. Bender, 'The kinetics of the alpha-chymotrypsin-catalyzed hydrolysis of p-nitrophenyl acetate', *Biochemistry* **1962**, *1*, 1097-1106.

[68] Y. Pocker, M. W. Beug, 'Kinetic studies of bovine carbonic anhydrase catalyzed hydrolyses of para-substituted phenyl esters', *Biochemistry* **1972**, *11*, 698-707.

[69] L. Anoardi, R. Fornasier, U. Tonellato, 'Functional Micellar Catalysis .4. Catalysis of Activated Ester Hydrolysis by Surfactant Systems as Chymotrypsin Models', *J. Chem. Soc., Perkin Trans. 2* **1981**, 260-265.

[70] J. H. Harvey, D. Trauner, 'Regulating enzymatic activity with a photoswitchable affinity label', *Chembiochem* **2008**, *9*, 191-193.